Journal of Geochemical Exploration 180 (2017) 101–112

Contents lists available at ScienceDirect

Journal of Geochemical Exploration

journal homepage: www.elsevier.com/locate/gexplo

Selenium and molybdenum enrichment in uranium roll-front deposits of Wyoming and Colorado, USA

Liam A. Bullock*, John Parnell

Dept. of Geology & Petroleum Geology, Meston Building, University of Aberdeen, King's College, Aberdeen, AB24 3UE, UK

ARTICLE INFO

Keywords:
Selenium
Molybdenum
Roll-fronts
Tellurium
Uranium
Wyoming

ABSTRACT

Sandstone uranium (U) roll-front deposits of Wyoming and Colorado (USA) are important U resources, and may provide a terrestrial source for critical accessory elements, such as selenium (Se), molybdenum (Mo), and tellurium (Te). Due to their associated toxicity, Mo–Se–Te occurrences in roll-fronts should also be carefully monitored during U leaching and ore processing. While elevated Mo–Se concentrations in roll-fronts are well established, very little is known about Te occurrence in such deposits. This study aims to establish Mo–Se–Te concentrations in Wyoming and Colorado roll-fronts, and assess the significance of these deposits in an environmental and mineral exploration context.

Sampled roll-front deposits, produced by oxidized groundwater transportation through a sandstone, show high Mo–Se content in specific redox zones, and low Te, relative to crustal means. High Se concentrations (up to 168 ppm) are restricted to a narrow band of alteration at the redox front. High Mo content (up to 115 ppm) is typically associated with the reduced mineralized nose and seepage zones of the roll-front, ahead of the U orebody. Elevated trace element concentrations are likely sourced from proximal granitic intrusions, tuffaceous deposits, and local pyritic mudstones. Elevated Mo–Se content in the sampled roll fronts may be regarded as a contaminant in U in-situ recovery and leaching processing, and may pose an environmental threat in groundwaters and soils, so extraction should be carefully monitored. The identification of peak concentrations of Mo–Se can also act as a pathfinder for the redox front of a roll-front, and help to isolate the U orebody, particularly in the absence of gamma signatures.

1. Introduction

Sandstone-type uranium (U) roll-front deposits of economic importance occur across Colorado and Wyoming in the United States (Jensen, 1958; Davis, 1969; Fischer, 1970; Childers, 1974; Dooley et al., 1974; Dahlkamp, 2010; Abzalov and Paulson, 2012, Owen et al., 2016). Uranium roll-front deposits (Fig. 1) are produced by groundwater transportation of dissolved elements in an oxidized fluid, with subsequent mineralization upon interaction with reducing agents (Harshman, 1974; Kesler, 1994; Abzalov, 2012). Uranium is leached from the original source rock, before being precipitated into the host porous sandstone. Geometrically, mineralization cross-cuts bedding, forming a characteristic crescent-shaped profile located between oxidized and reduced sandstone (Granger and Warren, 1969; Rubin, 1970; Abzalov, 2012; Fig. 1). Roll-front deposits also concentrate other trace elements, including selenium (Se) and molybdenum (Mo). While U has economic and environmental significance, Se, Mo, and other trace elements such as tellurium (Te) should also be considered critical trace elements, not only economically and environmentally, but could act as pathfinder elements for U exploration.

Enrichment of Mo–Se in roll-front deposits is well known, and a close association of Mo–Se–U has been previously documented (Harshman, 1974; Granger and Warren, 1978; Min et al., 2005; Abzalov, 2012). In conventional roll-front models, Se has a tendency to concentrate at the redox front, while Mo concentrates in reduced-unaltered sands (Harshman, 1966, 1974; Rubin, 1970; Spinks et al., 2014, 2016). However, understanding relating to redox-sensitive Te in roll-fronts is lacking, mainly due to analytical detection limitations. Enrichment of Te has been previously identified in continental red bed successions (Spinks et al., 2016; Parnell et al., 2016b), often in inclusions in sulfide minerals or in reduction spheroids. Parnell et al. (2016b) detailed Te concentrating in low-temperature sedimentary environments, controlled by redox variations, and noted a consistent enrichment of Te across red bed localities. This suggests that Te may concentrate as a ubiquitous process (e.g. controlled by microbial activity), and be enriched locally in sediments. Due to their close chemical

* Corresponding author.
E-mail address: liam.bullock@abdn.ac.uk (L.A. Bullock).

http://dx.doi.org/10.1016/j.gexplo.2017.06.013
Received 29 November 2016; Received in revised form 8 May 2017; Accepted 18 June 2017
Available online 19 June 2017
0375-6742/ © 2017 The Authors. Published by Elsevier B.V. This is an open access article under the CC BY license (http://creativecommons.org/licenses/BY/4.0/).

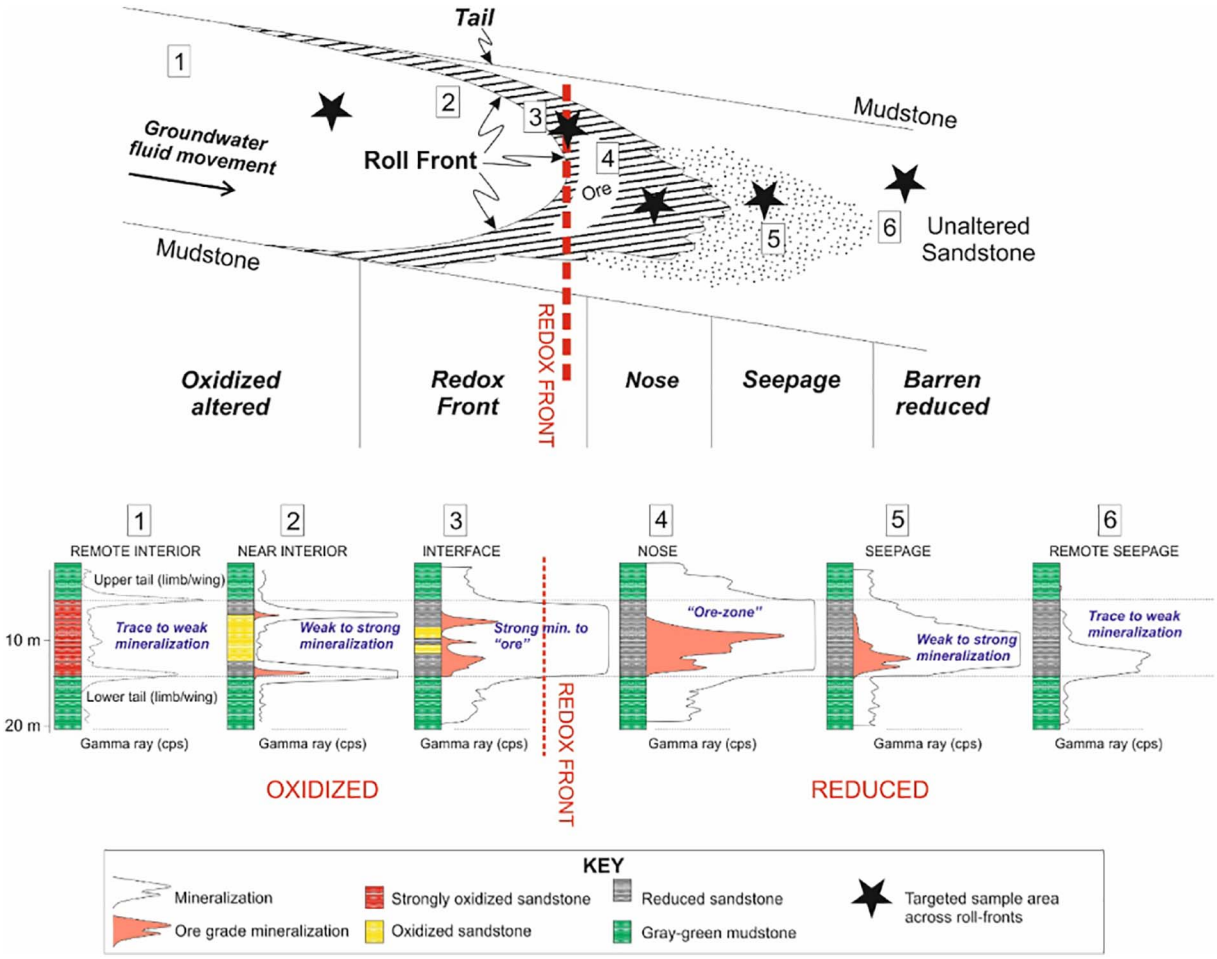

Fig. 1. Schematic cross-sectional illustration of a typical U roll-front deposit, with individual redox zone units and associated gamma signature shown (modified from Rubin, 1970). Oxidized groundwater fluid transports dissolved elements (that are mobile under oxidized conditions) through the sandstone, depositing elements at the redox front under reducing conditions. Sampled redox zones for this study also indicated.

affinities and redox-sensitive nature, it is therefore postulated that Te may also concentrate alongside Se in roll-front deposits, similar to Se—Te associations identified in red bed successions (Spinks et al., 2016; Parnell et al., 2016b). This study aims to establish if Mo—Se—Te are enriched in Wyoming and Colorado roll-fronts, and assesses the significance of these deposits in an environmental and mineral exploration context.

In high concentrations, Se and Mo are toxic and considered contaminants at U mine-waste sites (e.g. in United States sites, Dahlkamp, 2010; in Central Asia (Kazakhstan and Uzbekistan), Abzalov, 2012). High Mo—Se concentrations in weathered bedrock can have environmental ramifications, affecting livestock, groundwater, and soils (Fleming and Walsh, 1957; Legendre and Runnels, 1975; Rogers et al., 1990; Harris, 1992; Ramirez and Rogers, 2002; Alloway, 2012; Parnell et al., 2016a). Tellurium is also classified as a toxic trace element in high concentrations (Pohl, 2011; Schirmer et al., 2014), particularly in the form of tellurite (Templeton et al., 2000; El-Shahawi et al., 2013). Both Se and Te have also become elements of high economic interest, mainly due to their photovoltaic and photoconductive properties (Department for Environment, Food and Rural Affairs, DEFRA, 2012; Moss et al., 2011; Parnell et al., 2015a).

Here we report a data set covering four sandstone-hosted roll-front deposits across Colorado and Wyoming, comprising all redox zones (Fig. 1). This study will explore if Mo—Se—Te concentrations are significant in an environmental and/or mineral exploration context. High concentrations of Se in roll-fronts may provide a terrestrial critical metal resource (for instance, as a U by-product), while the lack of available data means that the Te source potential of roll-fronts is currently unknown. Furthermore, the sulfur (S) isotopic compositions of pyrite, where evident, were analyzed in order to indicate if microbial sulfate reduction was responsible for precipitation, as Se can replace (S) in metal sulfides.

2. Geological setting

The Denver Basin of Colorado, and the Cenozoic basins of Wyoming, host a number of economic sandstone U roll-front deposits (Craig, 1955; Harshman and Adams, 1980; Hopkins, 2002; Ur-Energy, 2016). The Great Divide Basin in Wyoming also hosts tabular U deposits, which commonly coexist in the same deposit as roll-front types. The roll-fronts often occur at depth, identified by drill hole gamma logs and drill core (Fig. 1), but may also be exposed at the surface. Examples include active Wyoming U subsurface projects in Shirley Basin (grid co-ordinates: 42.3224639, −106.869215), Hauber (grid co-ordinates: 44.7794286, −105.3802729), and Lost Creek (grid co-ordinates 42.0002345, −108.561221), all operated by Ur-Energy Inc., and exposed outcrop at Turkey Creek Road (Morrison, Colorado; Highway 285, grid co-ordinates: 39.634287, −105.170775) (Figs. 2–3). South eastern Wyoming samples were taken from core cuttings (part of active projects), and Colorado samples were collected at the surface (no exploration or mining activity). The anatomies of roll-fronts in Colorado and Wyoming exhibit a number of redox zones in cross section, including oxidized-altered sandstone, redox front (exhibiting both altered and reduced sandstone), nose (mineralized and reduced), near seepage (reduced)

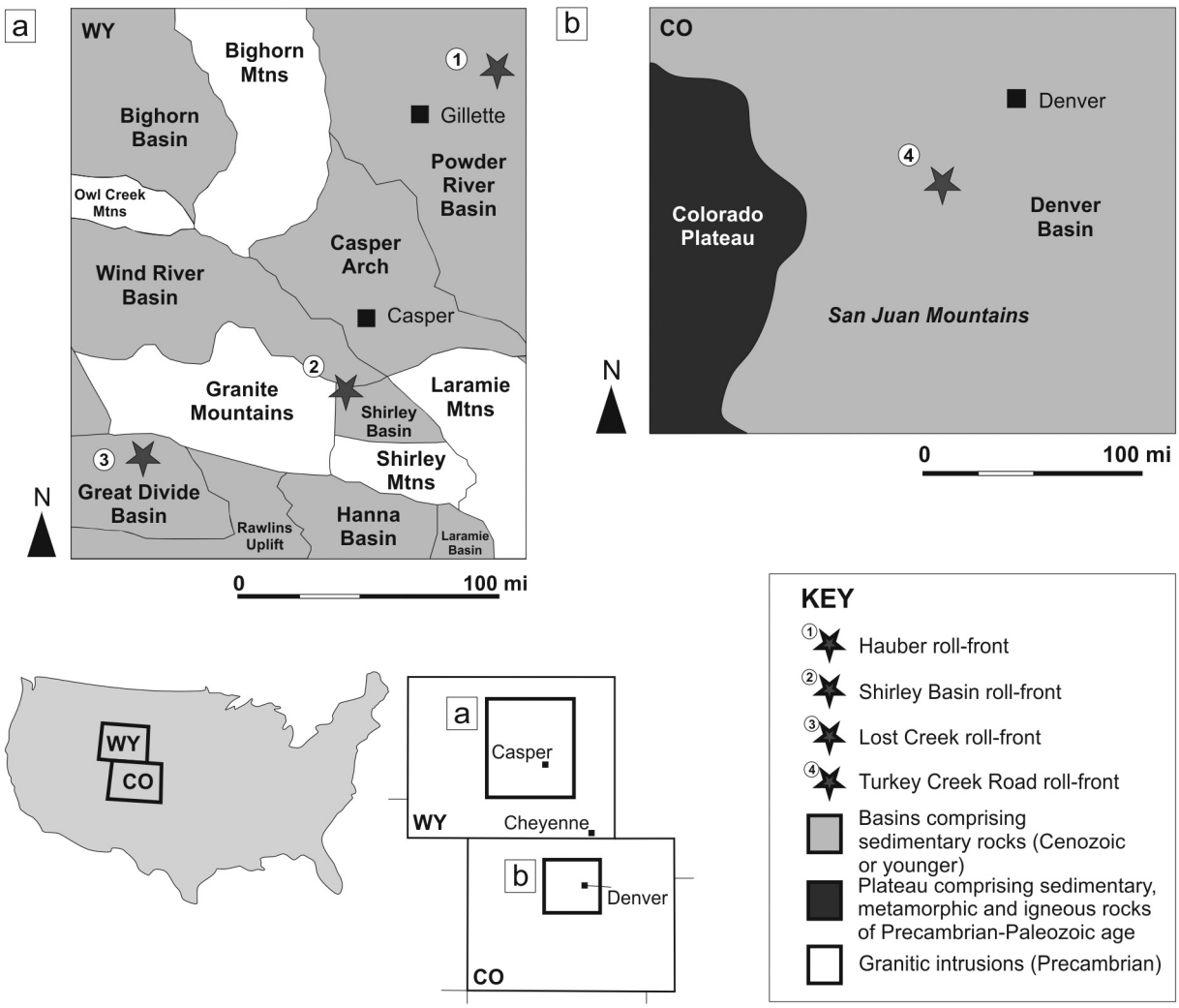

Fig. 2. Simplified map of sampled U roll-front deposit localities in (a) Wyoming and (b) Colorado, including associated basins, plateaus and igneous intrusive bodies (Modified from Blackstone, 1988; Snoke et al., 1993; Glass and Blackstone, 1999; Hopkins, 2002; Ur-Energy, 2016).

and barren reduced sandstone (Fig. 1).

The Wyoming area which hosts three of the sampled roll-fronts is characterized by late Paleozoic, Mesozoic and early Cenozoic basins, Precambrian granitic bodies, and Paleogene volcanic deposits. The older basement terranes are comprised of granitic intrusive units, Archean crystalline and metamorphic rocks, and a thick metasedimentary cover (Blackstone, 1988; Snoke et al., 1993; Glass and Blackstone, 1999). The granitic intrusions and basement rocks are evident at the Granite Mountains, the Laramie Mountains, and Bighorn Mountains (Fig. 2). These ranges represent the heavily eroded core of the intrusions, bound by normal faults. Paleozoic deposits are dominated by marine sediments (sandstone, mudstone, limestone, gypsum, and dolostone), with organic-rich marine sediments (shale) deposited during the Permian. Sediments were deposited throughout the Mesozoic era (development of the Wind River Basin and Great Divide Basin), with a period of volcanic activity occurred during the Cenozoic era depositing volcaniclastic rocks, lava flows, shallow intrusive bodies, and ash. The north of Shirley Basin hosts some of these Oligocene volcaniclastic rocks and Eocene sediments. The Powder River Basin and Hannah Basin are predominantly made up of Cenozoic sedimentary rocks (Blackstone, 1988; Snoke et al., 1993; Glass and Blackstone, 1999).

The Turkey Creek Road roll-front in Morrison is hosted within quartzose sandstone, forming part of the Lower Cretaceous Dakota Sandstone of the Denver Basin (Craig, 1955). The Denver Basin is characterized by late Cenozoic strata overlying folded Paleozoic and Mesozoic sediments. The Morrison region also hosts undifferentiated volcanic and intrusive igneous rocks of the Cenozoic Era (Hunt, 1956). The roll-front is exposed in a road cut (on both sides of the Turkey Creek Road), with clear divisions in oxidized, mineralized, and reduced zones evident (Fig. 3). Roll-fronts in both Wyoming and Colorado are bound above and below by gray-green mudstones.

3. Methodology

Samples were collected from four roll-front mineral occurrences: three from drill core at depths of approximately 200–400 ft. (Shirley Basin, Hauber and Lost Creek roll-fronts; Wyoming), and one sampled at the surface (Turkey Creek Road roll-front, Colorado) (Figs. 2–3). Mineralization in the subsurface roll-fronts of Wyoming that were sampled for this study were acquired and characterized by gamma logs and drill cores, as well as limited assay data (both collected by Ur-Energy). Roll-front U mineralization exhibits a characteristic gamma response (Fig. 1), based on the intensity of the naturally-occurring radioactivity emitted by U isotopes. The gamma ray scanning method (using a Geiger counter) measures the naturally occurring gamma radiation of uranium of a rock in a borehole, as different types of rock emit different radiation amounts and spectra. Gamma ray scanning also assists in distinguishing between bounding clays and the sandstone body. Turkey Creek Road samples acquired at the surface were selected

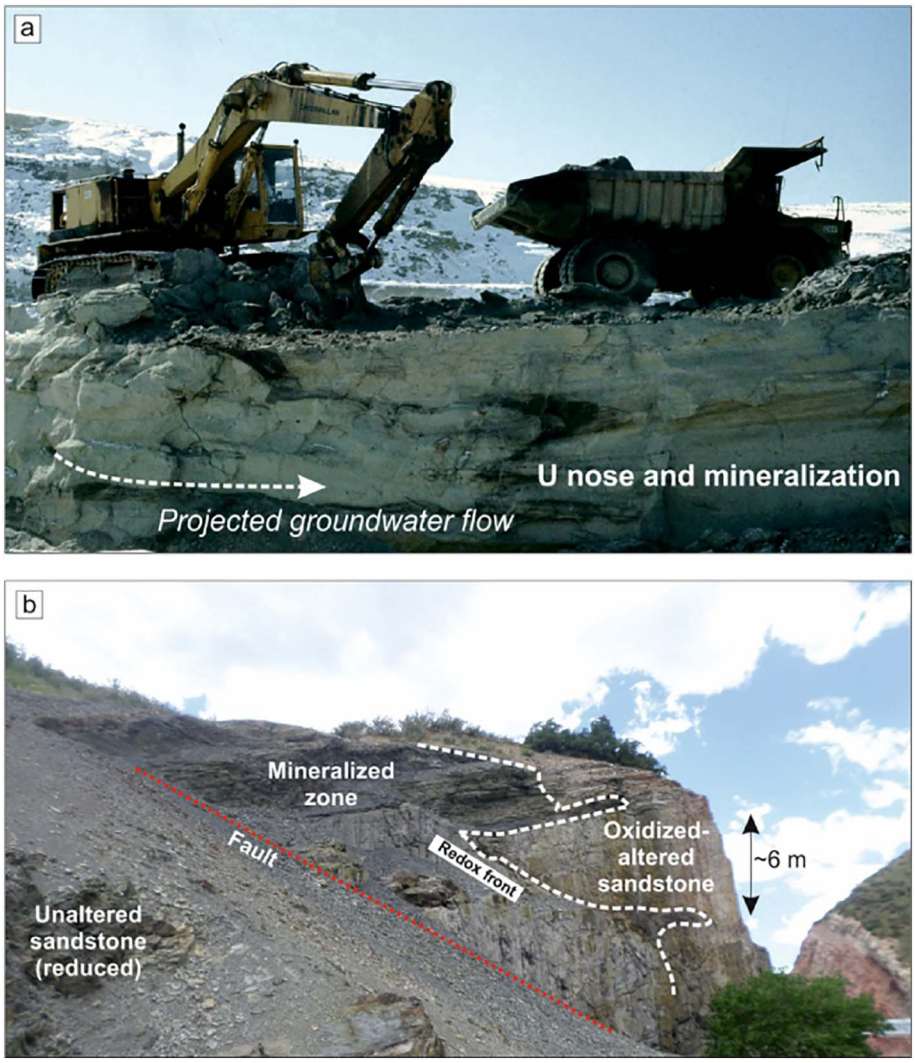

Fig. 3. Field images of two of the sampled roll-fronts exposed at the surface or shallow subsurface. (a) Sub-soil exposure of the Shirley Basin roll-front (with projected groundwater flow). (b) Road cut surface exposure of Turkey Creek Road roll-front.

based on their lithological appearance, i.e. color variations, differences in mineralogy, and organic content.

Sandstone samples were analyzed for trace element contents by inductively coupled plasma-mass spectrometry (ICP-MS). Samples of ~30 g rock were milled and homogenized, and 0.25 g were digested with aqua regia in a graphite heating block. The residue was diluted with deionized water, mixed, and analyzed using a Varian 725 instrument at ALS Minerals (Loughrea, Ireland and Reno, Nevada; ME-MS41). In some geological matrices, data reported from an aqua regia leach should be considered as representing the leachable portion of the analyte. Aqua regia digestion was chosen (as opposed to 4-acid digestion) in order to dissolve base metals, volatile elements, organic matter, sulfides, and carbonates, leaving behind the detrital silicate components. Aqua regia has been previously shown to be an efficient method for inferring paleoredox conditions, as the total amount of organic carbon and sulfur must be taken into account, while threshold values for trace metal ratios based on whole-rock (4-acid digest) compositions are not globally applicable to infer redox conditions (Xu et al., 2012). The 4-acid digestion is also deemed not suitable for rare earth elements, volatile elements, and some refractory minerals such as oxide minerals, as these are only partially digested. Samples with high concentrations were accordingly diluted, homogenized, and then analyzed by ICP-MS. Results were corrected for spectral inter-element interferences. Lower detection limits were: Mo (0.05 ppm), Se (0.01 ppm), Te (0.001 ppm), U (0.05 ppm) (see Supplementary material A5 for QA-QC). Error calculated (based on seven certified standards and one duplicate analysis) for each element are: Mo (6%), Se (10%), Te (13%), and U (11%) (Supplementary material A5).

Pyrite samples from selected roll-front zones (Turkey Creek Road seepage and oxidized zones, and Hulett Creek seepage zone) were prepared for conventional sulfur isotopic analysis by hand picking techniques. Pyrite samples were combusted with excess Cu_2O at 1075 °C in order to liberate the SO_2 gas under vacuum conditions. Liberated SO_2 gases were analysed on a VG Isotech SIRA II mass spectrometer, with standard corrections applied to raw $\delta^{66}SO_2$ values to produce true $\delta^{34}S$. Sulfur has five naturally occurring isotopes, four which are stable (^{32}S (95% terrestrial abundance), ^{33}S, ^{34}S, and ^{36}S), and ^{35}S is radiogenic. Stable isotope geochemistry is concerned primarily with the relative partitioning of stable isotopes among substances (i.e., changes in the ratios of isotopes), rather than their absolute abundances. The principal ratio of concern in sulfides is $^{34}S/^{32}S$, i.e. in the $\delta^{34}S$ notation, with units of parts per thousand or permil (‰) variations from the V-CDT standard (Bottrell et al., 1994; Seal, 2006). The standards employed were the international standards NBS-123 and IAEA-S-3 (supplied by the IAEA), and Scottish Universities Environment Research Centre (SUERC) laboratory standard CP-1. These gave $\delta^{34}S$ values of +17.1‰, −31.2‰ and −4.6‰ respectively, with 1σ reproducibility, based on repeat analyses of the standards, better than ± 0.2‰.

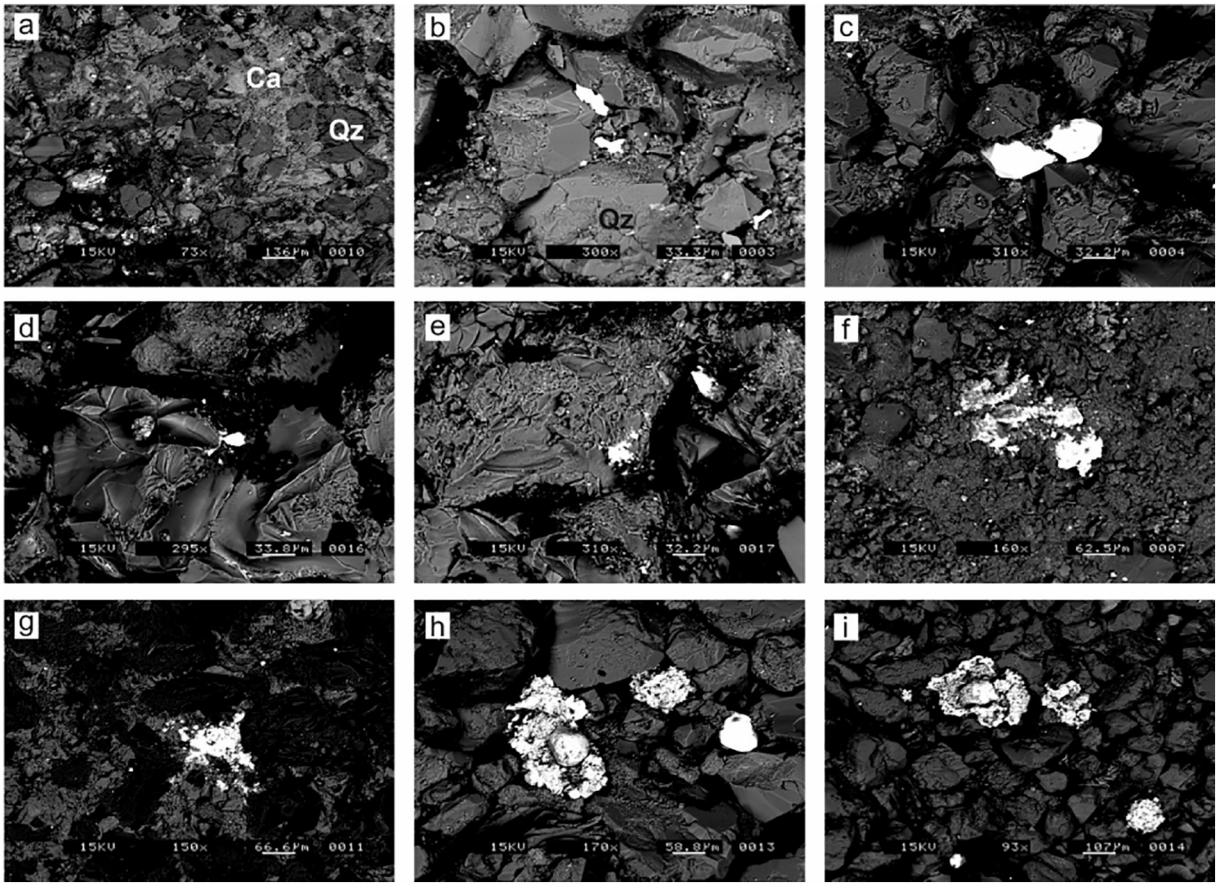

Fig. 4. Mineralogy of sampled roll-front deposits. (a) Calcitic cement in Hauber roll-front. (b) Cu-silicates in pore space. (c) Zircon in Hauber roll-front. (d) Fe- and Al-bearing uraniferous mineral (Turkey Creek Road roll-front). (e) U- and Mo-bearing silicate in Turkey Creek Road roll-front. (f) Coffinite in Shirley Basin roll-front. (g-i) Pyrite minerals in Hauber roll-front.

4. Results

All samples are typically compacted, poorly-sorted arkosic to well-sorted quartzitic sandstone (medium to coarse grained; Fig. 4). Oxidized-altered sandstone samples generally contain iron oxides (hematite and goethite). Ahead of the redox front, into the nose zone, samples contain nodular and concretionary pyrite, uraninite, coffinite, and some organic material. Roll-fronts are more highly mineralized in the nose, which represents the center (highest grade) of the U orebody. Barren reduced sandstone samples contain trace amounts of pyrite and rare organic matter. Roll-front samples often show a calcitic cement (Fig. 4a), Cu- and U-bearing minerals (Fig. 4b, e), zircon (Fig. 4c), and pyrite (Fig. 4g–i). Pyrite minerals sometimes show a framboidal habit. The most typically occurring U-bearing mineral in the sampled roll-fronts is coffinite, a U-silicate mineral that replaces organic matter in sandstones (Stieff et al., 1955). Coffinite occurs in association with pyrite, marcasite, and clay minerals in the roll-front samples, often in reduced zones (sometimes forming as an alteration product of uraninite). Another U-bearing mineral identified in samples occurs in association with Fe, Al, and S. This may be coconinoite (which typically favors oxidized zones), and is known to occur in other U-bearing rocks of Colorado, Utah, Arizona, and Wyoming (Anthony et al., 1995). The final U-bearing mineral in the roll-front samples is associated with Ca, which may be tyuyamunite, torbernite, or autunite, all previously identified in Wyoming (Weeks and Thompson, 1954). The mudstone and redox front units of all sampled roll-fronts in Wyoming and Colorado are variably pyritic, with active oil seepage and yellow sulfurous staining in reduced portions of the Turkey Creek Road roll-front.

Summary ICP-MS geochemical data for Mo—Se in Wyoming and Colorado roll-front deposits are shown in Table 1 and Figs. 5–6, with individual roll-front schematics shown in Fig. 7. All Mo—Se—Te—U data and QA-QC are available in the Supplementary materials. Concentrations of Te are generally low (below detection limit), and are thus omitted from Table 1 and Figs. 5–7. Overall, Se is low in concentrations in oxidized-altered sandstones (maximum of 0.7 ppm; average of 0.5 ppm), peaking in concentrations at the redox front (168 ppm behind the U orebody at Hauber roll-front), before tailing off to low amounts in unaltered primary reduced sandstones (maximum of 3.2 ppm; average of 0.6 ppm). Enrichment of Se (compared to an upper crustal mean of 0.05 ppm; Greenwood and Earnshaw, 2012) is higher at the redox front (Table 1, Fig. 7), and Se is generally enriched across all redox zones. The high Se concentrations at Hauber in the redox front are in close proximity to dark gray shales (i.e. just below the overlying shales). These samples contain pyrite and organic matter, and are a mixture of oxidized and reduced lithologies (gray green to reddish gray in color). The average Se content across all localities and zones is 13 ppm (n = 161), notably enriched compared to the crustal Se component. The redox front samples have the highest average Se content (57 ppm).

The average Mo content across all samples is 15 ppm (n = 161). The Mo enriched concentrations (compared to crustal average of 1.2 ppm; Pohl, 2011; Table 1) are more variable, with high concentrations ahead of the U orebody (i.e. in the nose and seepage zones; Fig. 7). The highest Mo concentration is 115 ppm in the Turkey Creek Road roll-front nose zone. Samples that show high Mo ahead of the U orebody are dark gray in color, fine- to medium-grained, and are commonly associated with recognizable organic matter and pyrite. In nose and seepage zone samples, Mo is typically higher than Se. The Hauber locality is enriched in Mo ahead of the redox front, with notably high Mo in the barren reduced sandstone. The Turkey Creek Road locality samples also show high Mo in the barren reduced sandstone samples ahead of the redox front. The nose zone generally favors high U content compared to the redox front (zone of high Se) and seepage

Table 1
Summary of Mo–Se content (ppm) across all sampled roll-fronts, within individual roll-fronts (characterized by redox zones).

	Oxidized-altered	Redox front	Nose	Seepage	Barren reduced
Overall (n = 161)					
Overall Se average	0.5	56.8	4.7	2.4	0.6
Overall Se max	0.7	167.5	19.4	31.9	3.2
Overall Mo average	–	13.4	13	19.8	2.6
Overall Mo max	–	61.4	114.5	89.9	22
Hauber (n = 70)					
Hauber Se average	–	52.6	7	2	–
Hauber Se max	–	167.5	19.4	31.9	–
Hauber Mo average	–	14.7	20.9	25.4	–
Hauber Mo max	–	61.4	83	65	22
Shirley Basin (n = 8)					
Shirley Basin Se average	–	52.1	6.3	–	–
Shirley Basin Se max	–	136	18.2	–	–
Shirley Basin Mo average	–	7.8	6.2	16.7	–
Shirley Basin Mo max	–	19	9	35.6	15
Lost Creek (n = 43)					
Lost Creek Se average	0.5	78.6	0.2	2.9	0.3
Lost Creek Se max	0.7	130	0.6	12.3	0.9
Lost Creek Mo average	0.2	0.9	0.2	0.4	0.3
Lost Creek Mo max	0.3	2	0.3	1	0.5
Turkey Creek Road (n = 5)					
Turkey Creek Road Se average	0.4	–	–	–	2.7
Turkey Creek Road Se max	0.5	33.8	1.9	11.7	3.2
Turkey Creek Road Mo average	3.2	–	–	–	1.5
Turkey Creek Road Mo max	5.7	60.2	114.5	89.9	1.7

(zone of high Mo) (Fig. 6).

Concentrations of Te are generally low across all roll-front samples, with most samples showing trace amounts (0.001–0.01 ppm) or concentrations below level of detection. Due to the low values and associated analytical error, some calculated Te concentrations may in reality be below detection level. The average measured Te content across all roll-front samples is 0.009 ppm (n = 46), with a maximum Te concentration of 0.1 ppm (coinciding with a relatively enriched Se content of 56.6 ppm). This maximum Te and enriched Se is from the upper confining zone (just below the overlying shale) of the Hauber roll-front, as previously mentioned.

The S isotopic values for pyrites extracted from the Turkey Creek seepage, Turkey Creek oxidized and Hauber seepage zones (n = 3) were − 32.6‰, − 21.1‰ and − 48.8‰ respectively. In all three cases, the pyrite S was found to have a ^{32}S–enriched (isotopically light) composition.

5. Discussion

5.1. Mo–Se–U source

Lost Creek roll-front sediments are sourced from Cenozoic rocks of the Hanna Basin. The Shirley Basin comprises the Eocene age porous sandstones (Wind River Formation) and Oligocene volcaniclastic rocks, while the Hauber sediments are sourced from Cretaceous and Cenozoic marine sedimentary rocks of the Powder River Basin. Turkey Creek Road roll-front sediments are sourced from the Denver Basin (Morrison Formation). Enrichment of Mo–Se typically accompanies U in these roll-front deposits, as all elements are redox-controlled. These trace elements likely originated from an igneous source, with the most probable source being either Early Proterozoic intrusions, or Middle Eocene and younger volcanic tuffs (Guilinger, 1963; Zielinski, 1983; Harris, 1984; Harris and King, 1993).

The most cited and probable sources for U and associated Mo–Se enrichment of roll-fronts in Wyoming are the granitic rocks and trachytic-rhyolitic tuff deposits of the south eastern Wyoming region (Harshman, 1972; Rosholt et al., 1973; Stuckless and Nkomo, 1978; Dahlkamp, 2010). The Granite Mountains, which are situated in between the Lost Creek and Shirley Basin roll-fronts (Fig. 2), and Laramie Range (plus tuffaceous sediments) provide a plausible proximal source of Mo–Se, particularly as U occurs as anomalous constituent of minerals within these rocks (Harris, 1984; Harris and King, 1993). The Granite Mountains and Laramie Range have been substantially eroded, which could provide the Mo–Se–U to the nearby basins (Guilinger, 1963; Harris, 1984; Harris and King, 1993). These trace elements were later mobilized in groundwater, percolating downwards and later precipitated to form the U orebody and related Mo–Se enrichment.

Rocks of the Granite, Laramie, and Shirley Mountain ranges (and sourced arkose rocks) contain up to 7 ppm leachable U (Harshman, 1972), with up to 30 ppm U in granites of the Sweetwater Uplift. Sweetwater Uplift granites also show substantial depletion of U (up to 75%) over the last 40 Ma, based on existing radiogenic lead amounts (Rosholt et al., 1973; Stuckless and Nkomo, 1978; Dahlkamp, 2010).

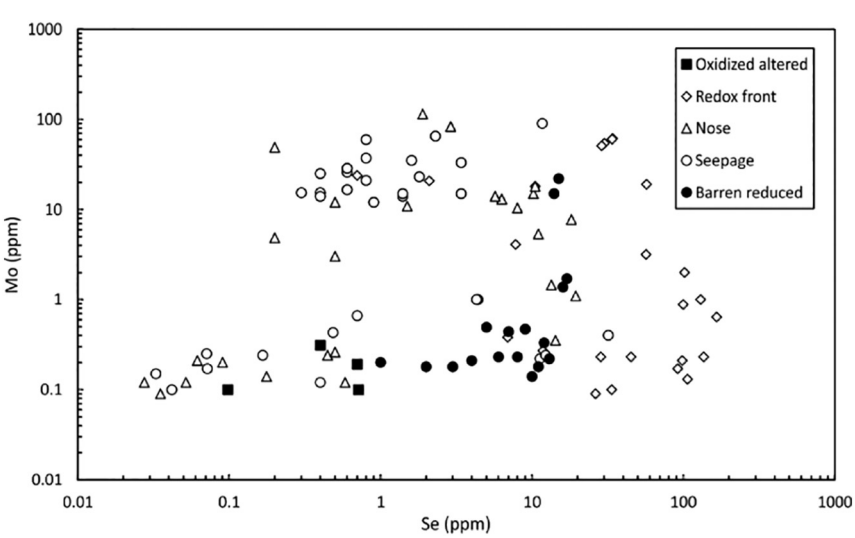

Fig. 5. Se and Mo content (ppm) of sampled roll-fronts, categorized by roll-front anatomy redox zones.

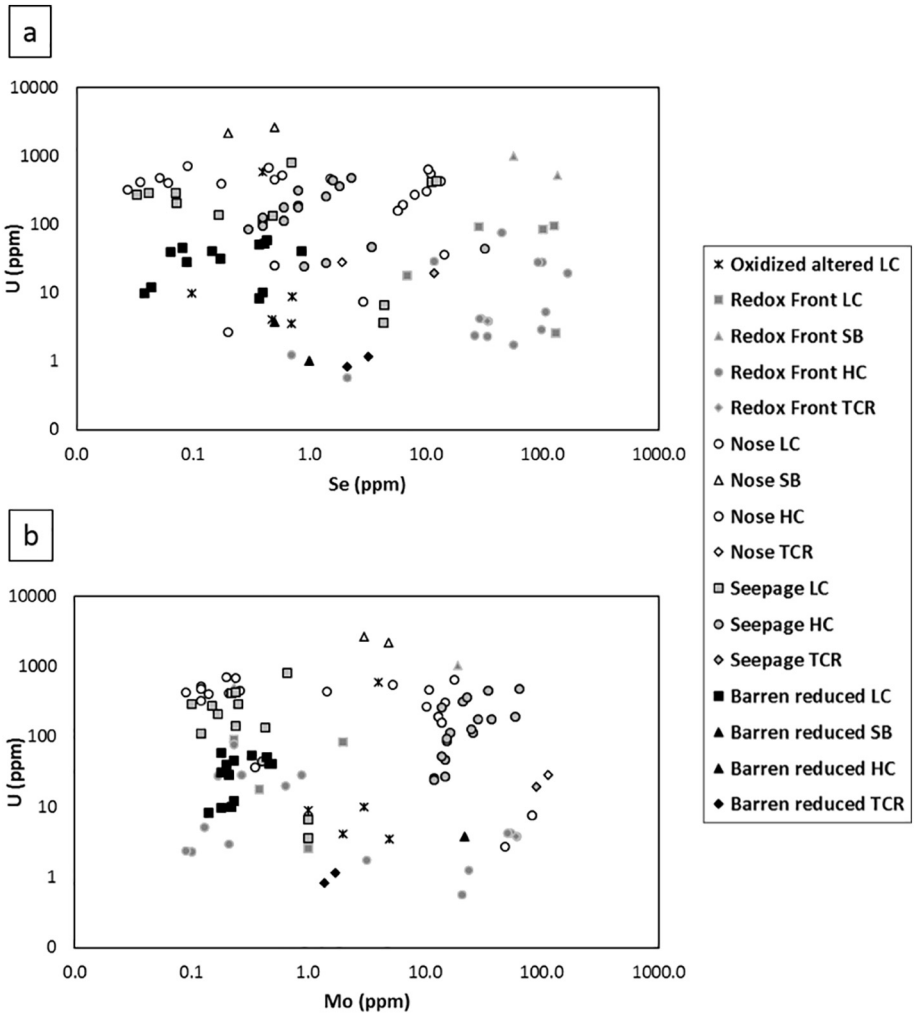

Fig. 6. U vs. (a) Se, and (b) Mo. LC = Lost Creek; SB = Shirley Basin; HC = Hauber; TCR = Turkey Creek Road. Cross symbols = oxidized-altered samples; light gray symbols = redox front; white symbols with black outline = nose; dark gray symbols with black outline = seepage; bold black symbols = barren reduced samples.

White River and Shirley Basin ash deposits also contain up to 250 ppm U in chalcedony (Zielinski, 1983). Middle and Upper Eocene Tuffaceous deposits of White River, Shirley Basin, and Freemont County host high Se concentrations, including up to 187 ppm water soluble Se in Freemont County (Davidson and Powers, 1959). The source for trace element enrichment in Morrison Formation sandstones and the Turkey Creek Road roll-front is likely to be the Colorado Plateau, where U deposits are well established (Hunt, 1956; Coleman and Delevaux, 1957). Up to 3 wt% of Se in pyrite in Colorado Plateau U deposits has been previously identified, with ferroselite, iron selenide, and clausthalite (PbSe) also found within these rocks (Coleman and Delevaux, 1957).

Another potential source (or means of Mo−Se enrichment) that has possibly been previously overlooked are the associated pyritic mudstone deposits in south eastern Wyoming. At the Hauber roll-front, the close proximity between high the Se concentrations (and more notable Te abundance) and overlying mudstones suggests that the mudstones may provide a source of trace element enrichment in this sandstone. Modern day hydromorphic dispersion likely plays an important role in the transport of trace elements from the near surface environment to the sampled roll-fronts. Present day river drainage does not indicate that the Bighorn Mountains provided the only source of trace elements to the Hauber roll-front. However, contemporary drainage (locally-derived) could provide a source of Mo−Se(−Te) to the Hauber roll-front. Selenium (and possibly Te) may have been leached from the overlying mudstones (mobilized by oxidized fluids), with downward propagation and re-deposition within the sandstone near the redox front (under reduced conditions). Mudstones from eastern Wyoming show elevated Mo−Se concentrations. For instance, Mo content of pyrite separates of the Green River Formation oil shales are 25–185 ppm (Harrison et al., 1973). The Pierre Shale (Upper Cretaceous) of Niobrara County contains anomalous Se (typically > 30 ppm) (Kulp and Pratt, 2004), while shales in Medicine Bow Formation (Albany County, south eastern Wyoming) contains over 150 ppm Se (Harrison et al., 1973). Niobrara shale of south eastern Wyoming contains up to 52 ppm Se, and shale beds associated with the Dakota Sandstone (Albany County) contain up to 10 ppm Se. These elevated Mo−Se mudstone concentrations suggest a potential locally-derived trace element source, or a possible means of trace element enrichment, in the Hauber roll-front.

5.2. Sulfur isotope composition

The ^{32}S–enriched isotope composition in pyritic zones of the Turkey Creek and Hauber roll-fronts are consistent with bacteriogenic pyrite, known to occur in other sandstones adjacent to sandstone-mudrock interfaces (Parnell et al., 2013). Here, porosity can accommodate microbes, and trace elements such as Mo−Se can diffuse from the mudrock (supporting a possible mudrock trace element source). The ^{32}S–enriched isotopic compositions compare well with other roll-front hosted sulfides in the United States (Spinks et al., 2016 and references therein). Isotopic compositions of Eocene roll-front samples from the Shirley Basin have been previously reported, ranging from −33 to +18‰ (Reynolds and Goldhaber, 1983). Eocene roll-fronts from Gas Hills (Wyoming) and Texas range from −52 to +10‰ and −33 to −20‰ respectively (Cheney and Trammell, 1973; Reynolds and Goldhaber, 1983). These results suggest that microbial activity plays a key role in

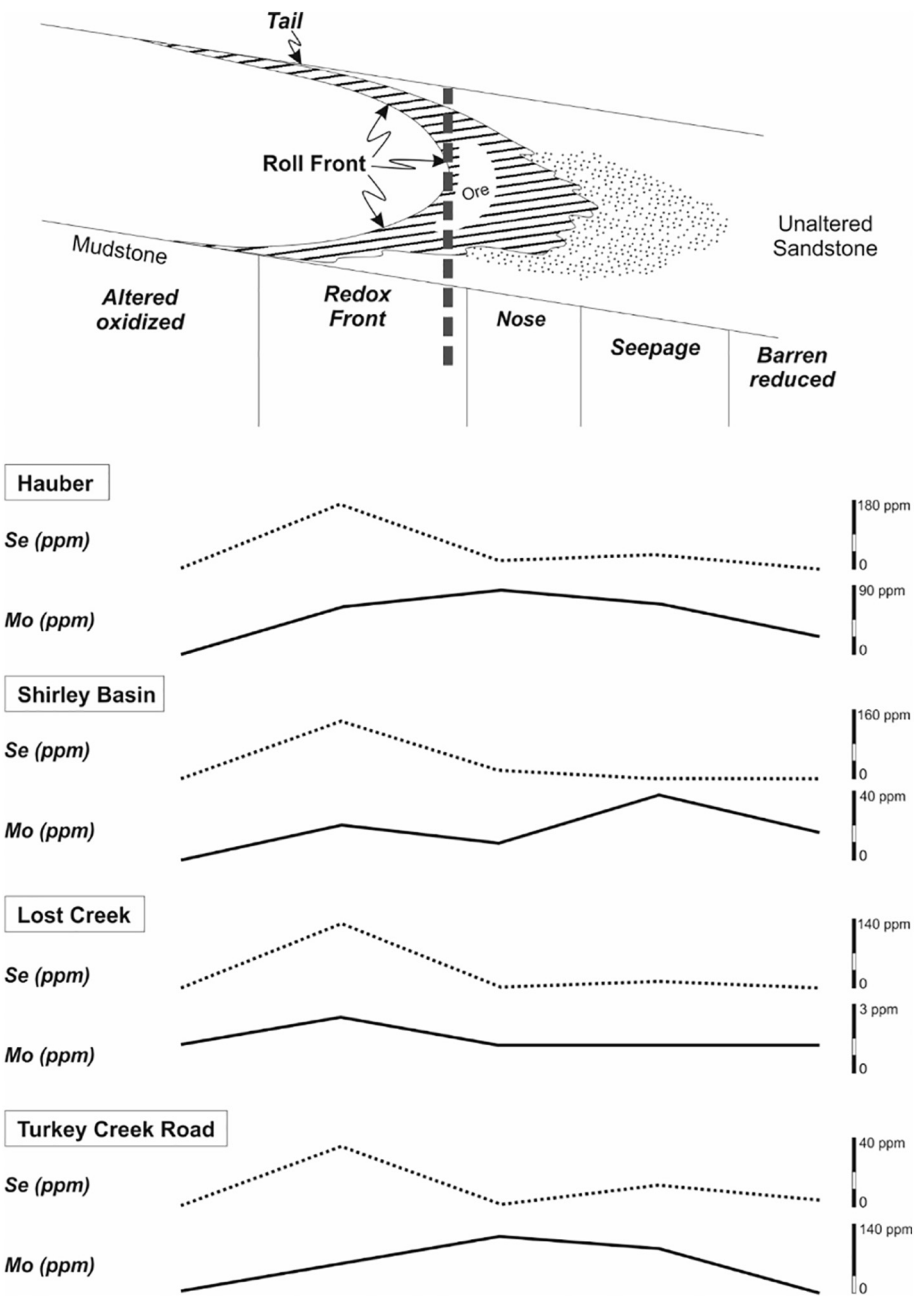

Fig. 7. Schematic representation of Se and Mo distribution in all sampled roll-front deposits through redox zones. Note higher Se content in redox front zone and higher Mo content in nose and seepage zones.

the specific distribution of Mo–Se in roll-fronts.

5.3. Mo–Se enrichment in roll-fronts

Uranium accumulates to form orebodies following oxidative U mobilization in groundwater, along with other redox-sensitive elements, including Mo–Se. The dissolved elements move downgradient within the hydrogeological regime, and precipitate across the redox front (Davidson, 1963; Harshman and Adams, 1980; Min et al., 2005; Abzalov, 2012; Spinks et al., 2014, 2016; Parnell et al., 2015a, 2015b, 2016b). At redox boundaries (across near-surface redox environments), Selenium requires oxidizing conditions to become mobile (Howard, 1977; Northrop and Goldhaber, 1990; Simon et al., 1997; Xiong, 2003; Min et al., 2005; Spinks et al., 2014, 2016). Variable oxidation states of Se mean that some Se species are more mobile than others, mainly due to the adsorption processes involving iron or manganese oxides, and clay minerals (Davidson, 1960; White and Dubrovsky, 1994). The soluble forms of Se include selenate (SeO_4^{2-}, +6 oxidation state and mobile in oxidizing conditions) and selenite (SeO_3^{2-}, +4 oxidation state). Selenium can occur in four oxidation states: II, III, IV, and VI (Luttrell, 1959; Davidson, 1960; Balistrieri and Chao, 1987; Burra, 2009). Selenium is typically mobilized as selenate, and precipitated under reducing conditions as elemental Se and metal selenides. Selenium-VI (as selenate) and selenium-IV (as selenite) are the predominant mobile forms, and selenides (Se^{2-}) and elemental selenium (Se^0) are insoluble (Davidson, 1960; Balistrieri and Chao, 1987).

In the sampled roll-fronts, selenate is likely to be reduced to metal Se^{2-} or Se^0 in the presence of a reducing agent (e.g. carbonaceous materials, sulfides, biogenic H_2S, ferromagnesian minerals) (Spinks et al., 2014, 2016). The strong adsorption tendency of selenite, and low solubility of Se^0 and Se (II) species mean that they are limited under reducing conditions. Originally, Se may have been present as selenide or partially substituting for sulfur in pyrite. Oxidation may have later altered selenide to Se^0, selenite, and later selenate, which is more limited under oxidizing conditions (Coleman and Delevaux, 1957; Davidson, 1960; Balistrieri and Chao, 1987; White and Dubrovsky,

1994). The speciation and/or mineral which hosts Se in the sampled roll-fronts is unknown, but may be in a selenide form, or in the observed pyrite and uraninite. Pyrite-uraninite deposits of other Wyoming Se-bearing U sandstones have been known to contain high concentrations of Se (Byers et al., 1938; Davidson, 1960), so it is plausible that Se in roll-fronts sampled in this study is hosted in pyrite-uraninite. The concentrated Se-rich zone observed across roll-fronts is formed by biogenically-induced reduction processes (Granger and Warren, 1969; Northrop and Goldhaber, 1990; Min et al., 2005; Yudovic and Ketris, 2006; Spinks et al., 2014, 2016; Parnell et al., 2015a, 2015b; Parnell et al., 2016a, 2016b), and the potential oxidative capacity of the fluids. As well as the presence of reducing agents and limited spatial distribution of anaerobic micro-organisms, the localized changes in electrochemically reducing (Eh) conditions and pH conditions may also promote concentrated Se zonation.

While high concentrations of Se are generally restricted to this envelope at the redox front, Mo concentrates ahead of the redox front and U orebody, in more heavily-reduced sandstone. The concentration of Mo further downgradient suggests that Mo requires strongly reducing conditions in order to precipitate, while Se (and U) can precipitate under less reducing conditions, closer to the redox front. Late, coarse, nodular, or concretionary pyrite is typical in the seepage zone of the roll-fronts, ahead of the U orebody, and may host Mo. Molybdenum requires lower Eh conditions to precipitate in the form of low soluble jordisite, MoS_2, and iron oxide minerals (Harshman, 1966, 1974; Harshman and Adams, 1980). The nose and seepage zones ahead of the redox front host the strongly reducing conditions required to promote Mo-bearing minerals and compounds, hence the higher concentrations of Mo in these zones ahead of the Se-rich zone and U orebody.

5.4. Te depletion in roll-fronts

Observed depletion of Te in the sampled roll-fronts may be due to a lack of Te from the source (or negligible role played by any Te-bearing rocks compared to Mo–Se–U source rocks), lack of mobility in oxidized fluids, and quartz dilution. Tellurium is known to concentrate in red bed successions, associated with low-temperature hydrothermal environments, controlled by redox variations and microbial activity (Afifi et al., 1988; Chapman et al., 2009; Spinks et al., 2016; Parnell et al., 2016b). Much like Se, Te commonly occurs in sulfide ores, replacing S^{2-} in anoxic systems (Pohl, 2011; Schirmer et al., 2014). Tellurium has also been shown to be enriched in organic-rich sediments (relative to a crustal mean of 0.001 ppm; Rudnick and Gao, 2003), together with Se (Large et al., 2014; Diehl et al., 2004). Due to these affinities, it may be anticipated that Te concentrates alongside Se in sampled roll-fronts. However, this is not the case, likely due to the lack of mobility of Te when compared to Se in oxidizing conditions, and the larger affinities of Te with iron hydroxides (Xiong, 2003; Harada and Takahashi, 2009; Schirmer et al., 2014; Parnell et al., 2015a), resulting in fractionation of Se and Te (Parnell et al., 2015a). Low Te concentrations and the Se/Te ratio of roll-front samples show significant Te depletion (compared to the average continental crust), with apparent Te depletion compared to other sedimentary deposits and settings (Fig. 8).

Depletion of Te may also be the result of variations in grain-size fractions in roll-front samples, which has been previously known to cause depletion of trace elements (Armstrong-Altrin et al., 2004). High Te content in argillaceous rocks has been attributed to adsorption onto fine clays (Beaty and Manuel, 1973), so an absence of such material within the roll-front as a whole may contribute to a lower Te content. Areas of the roll-front in close proximity to the (overlying and underlying) mudrocks may host higher Te content, as demonstrated by the slightly enriched Te content of 0.1 ppm in the Hauber roll-front sample (close to the overlying mudstone). Tellurium depletion may reflect dilution by higher quantities of coarser grained quartz and feldspar, with clay fractions preferentially leached and removed during groundwater transportation (Cullers et al., 1987; Cullers, 1988, 1994). In quartzose sandstones such as the sampled roll-fronts, a significant accumulation of heavy minerals is present (i.e. quartz). Therefore, depletion of trace elements such as Te may occur due to sedimentary sorting, loss of small grain fractions, and retention of sand-size compositions (Borges et al., 2008; Akarish and El-Gohary, 2011).

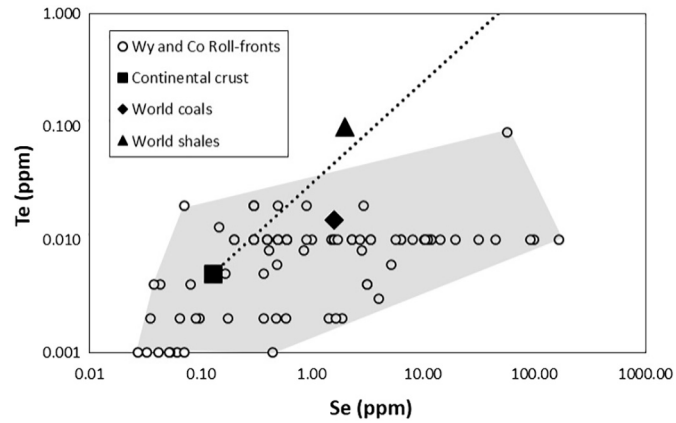

Fig. 8. Se/Te ratios of sampled roll-front deposits and various other geological settings (Davidson and Lakin, 1961; Rudnick and Gao, 2003). Dashed line represents continental crust Se/Te ratio (Rudnick and Gao, 2003; Hu and Gao, 2008) and gray shaded region shows extent of roll-front Se/Te values.

5.5. Implications for mineral exploration and the environment

Results for Mo–Se–Te concentrations in the sampled roll-fronts are low in an economic sense. Results demonstrate that, at least in the sampled areas, roll-fronts are not a viable source for Te. However, elevated Mo–Se concentrations (compared to the continental crust) are consistent with the well-established models of roll-front geochemical distribution (Adler and Sharp, 1967; Granger and Warren, 1969; Harshman, 1974; Eargle et al., 1975; Brookins, 1982; Boon, 1989; Spinks et al., 2014, 2016; Ruedig and Johnson, 2015), with important implications for environmental and exploration purposes. High Se content effectively shows the position of the redox front, and can be used to mark the interface between oxidized and reduced sandstones, while elevated Mo is a clear indicator of more reduced sediments (Fig. 9). Importantly, high U concentrations are consistently situated between spatial high Se and Mo concentrations, meaning Se and Mo peaks can be used as pathfinders to identify U orebodies (Figs. 6 and 9). This geochemical signature, coupled with a description of drill cuttings and gamma logs, provides a baseline method for identifying the location of U-rich deposits in roll-fronts.

As well as avoiding Mo–Se contamination during extraction and processing, it is important to avoid liberating and mobilizing these elements into the groundwater system, resulting in toxicity of plants, soils, and the food chain. It may therefore be necessary to identify and treat trace element contaminants during U mining and processing. Hydrometallurgical methods have been previously utilized to recover trace elements such as Mo–Se using acid leaching and alkali leaching (Zheng and Chen, 2014). Developments in biorecovery and microbiological processing can also focus on the isolation, identification, and selection of Mo-Se-reducing microorganisms, with optimal conditions for microbial bioreduction (Husen and Siddiqi, 2014). Because of the close spatial relationship of Mo–Se with U, it is virtually economically impossible to isolate the elements (or treat them separately) within any U mining method. However, careful monitoring and the recognition of their presence should be established. Release into groundwater or the environment is avoided by means of controlling mining solutions in the case of in-situ recovery, and by rigid control of tailings impoundments in the case of conventional mining.

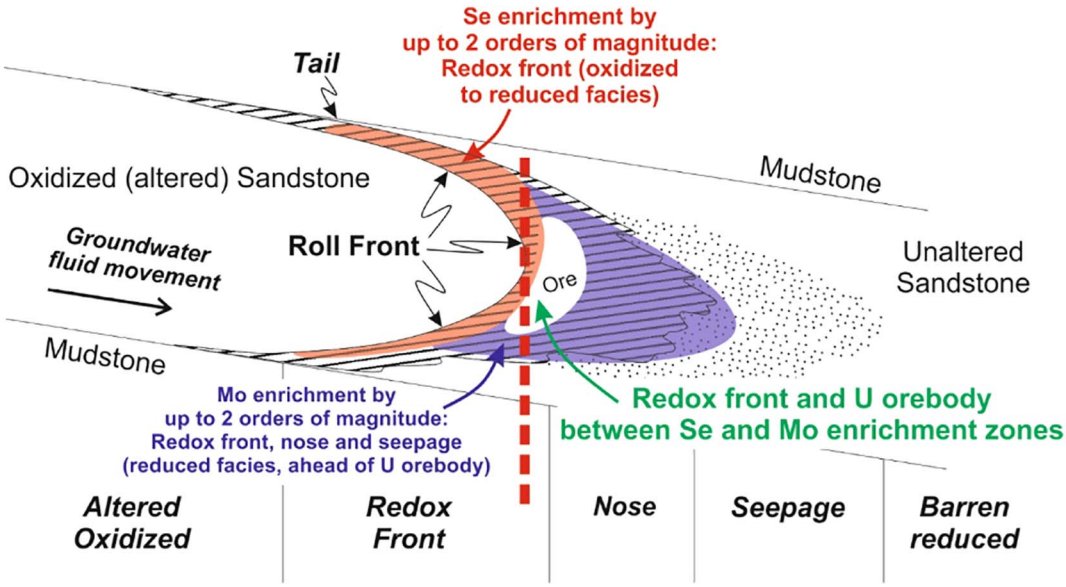

Fig. 9. Representative model of Mo–Se–U distribution in sampled Wyoming and Colorado roll-front deposits.

6. Conclusions

- Uranium roll-front deposits in Wyoming and Colorado show notably high Se (up to 168 ppm) and Mo (up to 115 ppm) concentrations, inferred to be sourced from proximal granitic intrusions, tuffaceous deposits, and locally pyritic mudstones (particularly in the case of the Hauber roll-front of Wyoming).
- Tellurium is depleted in roll-fronts with respect to the continental crust and other geological settings and deposits.
- High Mo–Se–U content relates to the initial mobilization of trace elements in oxidized conditions, and later precipitation down-gradient in reduced conditions.
- Enrichment of Mo–Se marks the redox front of the roll-front (Se) and heavily reduced (nose and seepage zone) sandstones (Mo). The consistent distribution of Mo–Se–U can be attributed to microbial activity, and their differing electrochemically reducing capacities.
- Elevated Mo–Se zoned concentrations can act as pathfinder elements, providing a general baseline survey to pinpoint the position of the U orebody in a roll-front.
- High Mo–Se concentrations should be carefully monitored during U leaching and ore processing due to the potential contamination effects and impact on the local groundwater system and soils.

Conflict of interest

The authors have no conflicts of interest to declare.

Funding

This research was supported by a grant from the Natural Environment Research Council (NERC) (NE/M010953/1).

Acknowledgements

The authors wish to thank Cal VanHolland, Jim Bonner and John Cooper of Ur-Energy (Casper, Wyoming) for their assistance with sampling, data provision, and feedback. We are grateful to Adrian Boyce and Alison McDonald of the Isotope Community Support Facility at SUERC for technical support with isotope sample preparation and analyses. Critical comments that greatly improved the manuscript from Samuel Spinks and Marat Abzalov are gratefully acknowledged.

Appendix A. Supplementary data

Supplementary data to this article can be found online at http://dx.doi.org/10.1016/j.gexplo.2017.06.013.

References

Abzalov, M.Z., 2012. Sandstone-hosted uranium deposits amenable for exploitation by in situ leaching technologies. Appl. Earth Sci. 121 (2), 55–64 *Transactions of the Institution of Mining and Metallurgy*, Section B.
Abzalov, M.Z., Paulson, O., 2012. Sandstone hosted uranium deposits of the Great Divide Basin, Wyoming, USA. Appl. Earth Sci. 121 (2), 76–83 *Transactions of the Institutions of Mining and Metallurgy*, Section B.
Adler, H.H., Sharp, B.J., 1967. Uranium ore rolls - occurrence, genesis and physical and chemical characteristics. In: Uranium Districts of Southeastern Utah; Guidebook to the Geology of Utah. 21. pp. 53–77.
Afifi, A.M., Kelly, W.C., Essene, E.J., 1988. Phase relations among tellurides, sulfides, and oxides: II. Applications to telluride-bearing ore deposits. Econ. Geol. 83, 395–404.
Akarish, A.I., El-Gohary, A.M., 2011. Pre-cenomanian sandstones, East Sinai, Egypt. J. Appl. Sci. 11 (17), 3070–3088.
Alloway, B.J., 2012. Heavy Metals in Soils. Springer, London.
Anthony, J.W., Williams, S.A., Bideaux, R.A., Grant, R.W., 1995. Mineralogy of Arizona, Third edn. The University of Arizona Press, Tuscon.
Armstrong-Altrin, J.S., Lee, Y.I., Verma, S.P., Ramasamy, S., 2004. Geochemistry of sandstones from the upper Miocene Kudankulam formation, southern India: Implications for provenance, weathering, and tectonic setting. J. Sediment. Res. 74 (2), 285–297.
Balistrieri, L.S., Chao, T.T., 1987. Selenium adsorption by goethite. Soil Sci. Soc. Am. J. 51, 1145–1151.
Beaty, R.D., Manuel, O.K., 1973. Tellurium in rocks. Chem. Geol. 12, 155–159.
Blackstone Jr., D.L., 1988. Traveler's Guide to the Geology of Wyoming (2nd Edition): *Wyoming State Geological Survey Bulletin* 67. (130 p).
Boon, D.Y., 1989. Potential Selenium Problems in Great Plains Soils. Soil Science Society of America Special Publication 23, Selenium in Agriculture and the Environment. pp. 107–121.
Borges, J.B., Huh, Y., Moon, S., Noh, H., 2008. Provenance and weathering control on river bed sediments of the eastern Tibetan Plateau and the Russian Far East. Chem. Geol. 254, 52–72.
Bottrell, S.H., Louie, P.K.K., Timpe, R.C., Hawthorne, S.B., 1994. The use of Stable Sulfur Isotope Ratio Analysis to Assess Selectivity of Chemical Analyses and Extractions of Forms of Sulfur in Coal. Fuel 73 (10), 1578–1582.
Brookins, D.G., 1982. Geochemistry of clay minerals for uranium exploration in the grants mineral belt, New Mexico. Mineral. Deposita 17 (1), 37–53.
Burra, R., 2009. Determination of selenium and tellurium oxyanion toxicity, detection of metalloid-containing headspace compounds, and quantification of metalloid oxyanions in bacterial culture media. In: Master of Science (Chemistry). Sam Houston State University, Huntsville, Texas (12/2009).
Byers, H.G., Miller, J.T., Williams, K.T., Lakin, H.W., 1938. Selenium Occurrences in Certain Soils in the United States with a Discussion of Related Topics. Third Report. U.S. Department of Agriculture Technical Bulletin No. 601. Department of Agriculture, Washington, DC, pp. 1–74.
Chapman, R.J., Leake, R.C., Bond, D.P.G., Stedra, V., Fairgrieve, B., 2009. Chemical and mineralogical signatures of gold formed in oxidizing chloride hydrothermal systems

and their significance within populations of placer gold grains collected during reconnaissance. Econ. Geol. 104, 563–585.
Cheney, E.S., Trammell, J.W., 1973. Isotopic evidence for inorganic precipitation of uranium roll ore bodies. Am. Assoc. Pet. Geol. Bull. 57, 1297–1304.
Childers, M.O., 1974. Uranium occurrences in Upper Cretaceous and Tertiary strata of Wyoming and northern Colorado. Mt. Geol. 11 (4), 131–147.
Coleman, R.G., Delevaux, M., 1957. Occurrence of selenium in sulfides from some sedimentary rocks of the western United States. Econ. Geol. 52, 499–527.
Craig, L.C., 1955. Stratigraphy of the Morrison and Related Formations, Colorado Plateau Region, A Preliminary Report. U.S. Geol. Surv. Bull. 1009-E, 125–168.
Cullers, R.L., 1988. Mineralogical and chemical changes of soil and stream sediment formed by intense weathering of the Danberg granite, Georgia, U.S.A. Lithos 21, 301–314.
Cullers, R.L., 1994. The controls on the major and trace element variation of shales, siltstones, and sandstones of Pennsylvanian-Permian age from uplifted continental blocks in Colorado to platform sediment in Kansas, USA. Geochim. Cosmochim. Acta 58 (22), 4955–4972.
Cullers, R.L., Barrett, T., Carlson, R., Robinson, R., 1987. Rare-earth element distributions in size fractions of Holocene soil and stream sediment, Wet Mountains region, Colorado, U.S.A. Chem. Geol. 63, 275–297.
Dahlkamp, F.J., 2010. Geology of the uranium deposits. In: Uranium Deposits of the World. Vol. 2 Springer, Verlag publisher, USA and Latin America (517 pp).
Davidson, D.F., 1960. Selenium in some epithermal deposits of antimony, mercury and silver and gold. U.S. Geol. Surv. Bull. 1112-A, 1–17.
Davidson, D.F., 1963. Selenium in some oxidized sandstone-type uranium deposits. U.S. Geol. Surv. Bull. 1162-C, C1–C33.
Davidson, D.F., Lakin, H.W., 1961. Metal content of some black shales of the western United States. U.S. Geol. Surv. Prof. Pap. 424, 329–331.
Davidson, D.F., Powers, H.A., 1959. Selenium content of some volcanic rocks from western United States and Hawaiian Islands. In: U.S. Geol. Surv. Bull. 1084-C (81pp).
Davis, J.F., 1969. Uranium deposits of the Powder River basin. In: Contributions to Geology, pp. 131–141 Wyoming Uranium Issue 8, (2), P1.
Department for Environment, Food & Rural Affairs (DEFRA), 2012. A Review of National Resource Strategies and Research. Department for Environment, Food and Rural Affairs, London.
Diehl, S.F., Goldhaber, M.B., Hatch, J.R., 2004. Modes of occurrence of mercury and other trace elements in coals from the warrior field, Black Warrior Basin, Northwestern Alabama. Int. J. Coal. Geol. 59, 193–208.
Dooley Jr., J.R., Harshman, E.N., Rosholt, J.N., 1974. Uranium-lead ages of the uranium deposits of the Gas Hills and Shirley Basin, Wyoming. Econ. Geol. 69, 527–531.
Eargle, D.H., Dickinson, K.A., Ogden Davis, B., 1975. South Texas uranium deposits. Am. Assoc. Pet. Geol. Bull. 59 (5), 766–779.
El-Shahawi, M.S., Al-Saidi, H.M., Al-Harbi, E.A., Bashammakh, A.S., Alsibbai, A.A., 2013. Speciation and determination of tellurium in water, soil, sediment and other environmental samples. In: Speciation Studies in Soil, Sediment and Environmental Samples, pp. 527–544.
Fischer, F.G., 1970. Similarities, differences, and some genetic problems of the Wyoming and Colorado Plateau types of uranium deposits in sandstones. Econ. Geol. 65, 778–784.
Fleming, G.A., Walsh, T., 1957. Selenium occurrence in certain Irish soils and its toxic effects on animals. Proceedings of the Royal Irish Academy. In: Section B: Biological, Geological, and Chemical Science. 58B. pp. 151–166.
Glass, G.B., Blackstone Jr., D.L., 1999. Geology of Wyoming: Wyoming State Geological Survey Information Pamphlet No. 2. (12 p).
Granger, H.C., Warren, C.G., 1969. Unstable sulfur compounds and the origin of roll-type uranium deposits. Econ. Geol. 64 (2), 160–171.
Granger, H.C., Warren, C.G., 1978. Some speculations on the genetic geochemistry and hydrology of roll-type uranium deposits. In: 30th Annual Conference, Wyoming Geological Association Guidebook, pp. 349–361.
Greenwood, N.N., Earnshaw, A., 2012. Chemistry of the Elements, 2nd Edition. Elsevier.
Guilinger, R.R., 1963. Source of uranium in the Gas Hills area, Wyoming: Econ. Geol. 58 (2), 285–286.
Harada, T., Takahashi, Y., 2009. Origin of the difference in the distribution behavior of tellurium and selenium in a soil-water system. Geochim. Cosmochim. Acta 72, 1281–1294.
Harris, R.E., 1984. Alteration and mineralization associated with sandstone uranium occurrences, Morton Ranch area, Wyoming. In: WSGS Report of Investigations No. 25.
Harris, R.E., 1992. Industrial minerals and construction materials of Wyoming. The Geological Survey of Wyoming. Reprint No. 50.
Harris, R.E., King, J.K., 1993. Geological classification and origin of radioactive mineralization in Wyoming. In: Snoke, A.W., Steidtman, J.R., Roberts, S.M. (Eds.), Geology of Wyoming: Geological Survey of Wyoming Memoir. 5. pp. 898–916.
Harrison, W.J., Pevear, D.R., Lindahl, P.C., 1973. Trace elements in pyrites of the Green River Formation oil shales, Wyoming, Utah, and Colorado. In: Tuttle, M.L. (Ed.), Geochemical, Biogeochemical, and Sedimentological Studies of the Green River Formation, Wyoming, Utah, and Colorado. US Geological Survey Bulletin (1973-D1-D23).
Harshman, E.N, 1966. Genetic implications of some elements associated with uranium deposits, Shirley Basin, Wyoming. In: Geological Survey Research 1966. U.S. Geol. Surv. Prof. Pap 550-C. pp. C167–C173.
Harshman, E.N., 1972. Geology and Uranium Deposits, Shirley Basin area, Wyoming: U.S. Geol. Surv. Prof. Pap. 745. pp. 82.
Harshman, E.N., 1974. Distribution of elements in some roll-type uranium deposits. In: Formation of Uranium Ore Deposits, International Atomic Energy Agency, pp. 169–183.
Harshman, E.N., Adams, S.S., 1980. Geology and recognition criteria for roll-type uranium deposits in continental sandstones. United States Department of Energy Report GJBX-1 (81).
Hopkins, R.L., 2002. Hiking the Southwest's Geology: Four Corners Region. Hiking Geology, Mountaineers Books, 1st Edition. .
Howard, J.H., 1977. Geochemistry of selenium: formation of ferroselite and selenium behavior in the vicinity of oxidizing sulfide and uranium deposits. Geochim. Cosmochim. Acta 41, 1665–1678.
Hu, Z., Gao, S., 2008. Upper crustal abundances of trace elements: a revision and update. Chem. Geol. 253 (3), 205–221.
Hunt, C.B., 1956. Cenozoic Geology of the Colorado Plateau. U.S. Geol. Surv. Prof. Pap. 279.
Husen, A., Siddiqi, K.S., 2014. Plants and microbes assisted selenium nanoparticles: characterization and application. Journal of Nanobiotechnology 12, 28.
Jensen, M.L., 1958. Sulfur isotopes and the origin of sandstone-type uranium deposits. Econ. Geol. 53, 589–616.
Kesler, S.E., 1994. Mineral Resources, Economics and the Environment. Macmillan College Publishing Company, Inc.
Kulp, T.R., Pratt, L.M., 2004. Speciation and weathering of selenium in Upper Cretaceous chalk and shale from South Dakota and Wyoming, USA. Geochemica et Cosmochimica Acta 68 (18), 3687–3701.
Large, R.R., Halpin, J.A., Danyushevsky, L.V., Maslennikov, V.V., Bull, S.W., Long, J.A., Gregory, D.D., Lounejeva, E., Lyons, T.W., Sack, P.W., McGoldrick, P.J., Calver, C.R., 2014. Trace element content of sedimentary pyrite as a new proxy for deep-time ocean–atmosphere evolution. Earth Planet Sci. Lett. 389, 209–220.
Legendre, G.R., Runnels, D.D., 1975. Removal of dissolved molybdenum from wastewater by precipitates of ferric iron. > Environ. Sci. Technol. 9, 744–748.
Luttrell, G.W, 1959. Annotated bibliography on the geology of selenium. In: US Geological Survey: Contributions to Bibliography of Mineral Resources. U.S. Geol. Surv. Bull. Washington United States Printing Office, pp. 1019-M.
Min, M., Xu, H., Chen, J., Fayek, M., 2005. Evidence of uranium biomineralization in sandstone-hosted roll-front uranium deposits, northwestern China. Ore Geol. Rev. 26, 198–206.
Moss, R.L., Tzimas, E., Kara, H., Willis, P., Kooroshy, J., 2011. Critical Metals in Strategic Energy Technologies. Publications Office of the European Union, Luxembourg.
Northrop, H.R., Goldhaber, M.B., 1990. Genesis of the tabular-type vanadium–uranium deposits of the Henry Basin, Utah. Econ. Geol. 85, 215–269.
Owen, A., Hartley, A.J., Weissmann, G.S., Nichols, G.J., 2016. Uranium distribution as a proxy for basin-scale fluid flow in distributive fluvial systems, J. Geol. Soc. 173 (4), 569–572.
Parnell, J., Boyce, A.J., Hurst, A., Davidheiser-Kroll, B., Ponicka, J., 2013. Long term geological record of a global deep subsurface microbial habitat in sand injection complexes. Sci. Rep. 3, 1828.
Parnell, J., Bellis, D., Feldmann, J., Bata, T., 2015a. Selenium and tellurium enrichment in palaeo-oil reservoirs. J. Geochem. Explor. 148, 169–173.
Parnell, J., Spinks, S., Andrews, S., Thayalan, W., Bowden, S., 2015b. High molybdenum availability for evolution in a Mesoproterozoic lacustrine environment. Nat. Commun. 6, 6996.
Parnell, J., Brolly, C., Spinks, S., Bowden, S., 2016a. Selenium enrichment in Carboniferous Shales, Britain and Ireland: Problem or opportunity for shale gas extraction? Appl. Geochem. 66, 82–87.
Parnell, J., Spinks, S., Bellis, D., 2016b. Low-temperature concentration of tellurium and gold in continental red bed successions. Terra Nova 28 (3), 221–227.
Pohl, W., 2011. Economic Geology: Principles and Practice. Wiley-Blackwell Publishing, UK.
Ramirez Jr., P., Rogers, B., 2002. Selenium in a Wyoming grassland community receiving wastewater from an in situ uranium mine. Arch. Environ. Contam. Toxicol. 42 (4), 431–436.
Reynolds, R.L., Goldhaber, M.B., 1983. Iron disulfide minerals and the genesis of roll-type uranium deposits. Econ. Geol. 78, 105–120.
Rogers, P.A.M., Arora, S.P., Fleming, G.A., Crinion, R.A.P., McLaughlin, J.G., 1990. Selenium toxicity in farm animals: treatment and prevention. Ir. Vet. J. 43, 151–153.
Rosholt, J.N., Zartman, R.E., Nkomo, I.T., 1973. Pb-isotope systematics and uranium depletion in the Granite Mountains, Wyoming. Geol. Soc. Am. Bull. 84, 989–1002.
Rubin, B., 1970. Uranium roll front zonation in the Southern Powder River Basin, Wyoming. Wyoming Geological Association Earth Science Bulletin 3 (4), 5–12.
Rudnick, R.L., Gao, S., 2003. Composition of the continental crust. In: Holland, H.D., Turekian, K.K., Rudnick, R.L. (Eds.), The Crust. Treatise on Geochemistry 3. Elsevier Pergamon, Oxford, pp. 1–64.
Ruedig, E., Johnson, T.E., 2015. An evaluation of health risk to the public as a consequence of in situ uranium mining in Wyoming, USA. J. Environ. Radioact. 150, 170–178.
Schirmer, T., Koschinsky, A., Bau, M., 2014. The ratio of tellurium and selenium in geological material as a possible paleo-redox proxy. Chem. Geol. 376, 44–51.
Seal II, R.R., 2006. Sulfur Isotope Geochemistry of Sulfide Minerals. U.S. Geol. Surv. Staff - Published Research Paper 345.
Simon, G., Kesler, S.E., Essene, E.J., 1997. Phase relations among selenides, sulfides, tellurides, and oxides: II. Applications to selenide-bearing ore deposits. Econ. Geol. 92, 468–484.
Snoke, A.W., Steidtmann, J.R., Roberts, S.M. (Eds.), 1993. Geology of Wyoming: Wyoming State Geological Survey Memoir No. 5. vols. 1–2.
Spinks, S.C., Parnell, J., Still, J.W., 2014. Redox-controlled selenide mineralization in the Upper Old Red Sandstone. Scott. J. Geol. 50, 173–182.
Spinks, S.C., Parnell, J., Bellis, D., Still, J., 2016. Remobilization and mineralization of selenium–tellurium in metamorphosed red beds: evidence from the Munster Basin, Ireland. Ore Geol. Rev. 72, 114–127.

Stieff, L.R., Stern, T.W., Sherwood, A.M., 1955. Preliminary description of coffinite – a new uranium mineral. Science 121, 608–609.
Stuckless, J.S., Nkomo, I.T., 1978. Uranium-lead isotope systematics in uraniferous alkali-rich granites from the Granite Mountains, Wyoming; implications for uranium source rocks. Econ. Geol. 73 (3), 427–441.
Templeton, D.M., Ariese, F., Cornelis, R., Danielsson, L.G., Muntau, H., van Leeuwen, H.P., Lobinski, R., 2000. Guidelines for terms related to chemical speciation and fractionation of elements. Definitions, structural aspects, and methodological approaches (IUPAC Recommendations 2000). Pure Appl. Chem. 72 (8), 1453–1470.
Ur-Energy, 2016. Shirley Basin Mine Site - Shirley Basin, Wyoming. http://www.ur-energy.com/shirley-basin/ (Accessed: 10/01/2017).
Weeks, A.D., Thompson, M.E., 1954. Identification and occurrence of uranium and vanadium minerals from the Colorado Plateaus. United States Geological Survey Bulletin 1009-B.
White, A.F., Dubrovsky, N.M., 1994. Chemical oxidation-reduction controls on selenium mobility in groundwater systems. In: Frankenberger, W.T., Benson, S. (Eds.), Selenium in the Environment. Marcel Dekker, Inc., New York, pp. 185–221.
Xiong, Y.L., 2003. Predicted equilibrium constants for solid and aqueous selenium species to 300 °C: applications to selenium-rich mineral deposits. Ore Geol. Rev. 23, 259–276.
Xu, G., Hannah, J.L., Bingen, B., Georgiev, S., Stein, H.J., 2012. Digestion methods for trace element measurements in shales: paleoredox proxies examined. Chem. Geol. 324-325, 132–147.
Yudovic, Y.E., Ketris, M.P., 2006. Selenium in coal: a review. Int. J. Coal Geol. 67, 112–126.
Zheng, Y.-J., Chen, K.-K., 2014. Leaching kinetics of selenium from selenium – tellurium-rich materials in sodium sulfite solutions. Trans. Nonferrous Metals Soc. China 24, 536–543.
Zielinski, R.A., 1983. Tuffaceous sediments as source rocks for uranium: a case study of the White River Formation, Wyoming. J. Geochem. Explor. 18 (3), 285–306.